Available online at www.sciencedirect.com
ScienceDirect
Biochimica et Biophysica Acta 1757 (2006) 1122–1132
BIOCHIMICA ET BIOPHYSICA ACTA
BBA
www.elsevier.com/locate/bbabio

Single-electron photoreduction of the P_M intermediate of cytochrome *c* oxidase

Sergey A. Siletsky [a,1], Dan Han [b,1,2], Sue Brand [c], Joel E. Morgan [b,3], Marian Fabian [d], Lois Geren [c], Francis Millett [c], Bill Durham [c], Alexander A. Konstantinov [a], Robert B. Gennis [b,*]

[a] *A.N.Belozersky Institute of Physico-Chemical Biology, Moscow State University, Moscow 119 992, Russia*
[b] *Department of Biochemistry, University of Illinois at Urbana-Champaign, Urbana, IL 61801, USA*
[c] *Department of Chemistry and Biochemistry, University of Arkansas, Fayetteville, AK 72701, USA*
[d] *Department of Biochemistry and Cell Biology, MS 140, Rice University, 6100 Main, Houston, TX 77005, USA*

Received 3 May 2006; received in revised form 13 July 2006; accepted 19 July 2006
Available online 21 July 2006

Abstract

The $P_M \rightarrow F$ transition of the catalytic cycle of cytochrome *c* oxidase from bovine heart was investigated using single-electron photoreduction and monitoring the subsequent events using spectroscopic and electometric techniques. The P_M state of the oxidase was generated by exposing the oxidized enzyme to CO plus O_2. Photoreduction results in rapid electron transfer from heme a to oxoferryl heme a_3 with a time constant of about 0.3 ms, as indicated by transients at 605 nm and 580 nm. This rate is ~5-fold more rapid than the rate of electron transfer from heme a to heme a_3 in the $F \rightarrow O$ transition, but is significantly slower than formation of the F state from the P_R intermediate in the reaction of the fully reduced enzyme with O_2 to form state F (70–90 μs). The ~0.3 ms $P_M \rightarrow F$ transition is coincident with a rapid photonic phase of transmembrane voltage generation, but a significant part of the voltage associated with the $P_M \rightarrow F$ transition is generated much later, with a time constant of 1.3 ms. In addition, the $P_M \rightarrow F$ transition of the *R. sphaeroides* oxidase was also measured and also was shown to have two phases of electrogenic proton transfer, with τ values of 0.18 and 0.85 ms.

Keywords: Bioenergetic; Oxidase; Photoreduction; Electrogenic; Electron transfer; Proton transfer

1. Introduction

There is growing evidence, in accordance with the initial models (e.g. [1,2]), that each of the four 1-electron transfers to the active site of cytochrome *c* oxidase during the reduction of O_2 to H_2O is coupled to the pumping of one proton across the membrane (N-side to P-side) [3–6]. Prominent current models of proton pumping make this assumption [6–10]. The chemistry of the reaction also requires, as postulated initially by Mitchell [11], that the transfer or each electron from cytochrome *c* (from the P side of the membrane) is coupled to the transfer of one proton to the oxygen-reducing site, and this proton comes from the opposite side of the membrane (the N-side). Hence, each electron transfer to the active site results in the net transfer of two elementary charges across the membrane, one charge associated with the chemistry and the second charge due to the proton pumping.

The chemistry occurring at the active site for each of the 4 steps is different [7,12–14], raising the possibility of differences in the details of the coupling mechanism between electron transfer and the proton pump. Hence, it is worthwhile to study each of the 4 four electron transfers required to reduce O_2 to H_2O individually. Such an approach is also experimentally

Abbreviations: RuBpy, tris-bipyridyl complex of Ru(II); Ru_2C, [Ru(bipyridine)$_2$]$_2$(1,4-bis[2-(4′-methyl-2, 2′-bipyrid-4-yl)ethenyl]benzene); 3-CP, 3-carboxy-2,2,5,5,tetramethyl-1-pyrrolidinyloxy free radical

* Corresponding author. Tel.: +1 217 333 9075; Fax: +1 217 244 3186.
E-mail address: r-gennis@uiuc.edu (R.B. Gennis).

[1] This is to indicate that these two authors made equal contributions to the work.

[2] Current address: 1700 4th Street, Building QB3, Room 204, Box 2520, University of San Francisco, CA, 94158, USA.

[3] Current address: Department of Biology, Center for Biotechnology and Interdisciplinary Studies, Room 2237, Rensselaer Polytechnic Institute, 110 Eighth St. Troy, NY 12180.

0005-2728/$ - see front matter © 2006 Elsevier B.V. All rights reserved.
doi:10.1016/j.bbabio.2006.07.003

advantageous since the events associated with individual steps can be isolated and identified. Starting with the oxidized enzyme, O, the sequence of electron transfers can be written as follows, where E, R, P_M and F are intermediate states of the active site.

$$O(+e^-)\rightarrow E(+e^-)\rightarrow R(+O_2)\rightarrow P_M(+e^-)\rightarrow F(+e^-)\rightarrow O$$

Each of these intermediates represents a different state of the oxygen-reducing active site of cytochrome oxidase. The active site of the oxidase includes the heme a_3/Cu_B bimetallic center as well as a tyrosine (Y244 in the bovine enzyme) which is essential for catalysis [15–18]. The enzyme also contains two additional redox centers, heme a and Cu_A, which provide a conduit for electrons from cytochrome *c* to get to the oxygen-reducing site. The enzyme will not react with O_2 until the binuclear site of the enzyme has been reduced by two electrons. The product of the reaction of O_2 with the 2-electron reduced enzyme is the P_M state (see Fig. 1) [12,19]. The O − O bond is split in this reaction, which requires the transfer of four electrons and at least one proton from the active site moieties to the O_2. Two electrons are provided by heme a_3 Fe^{2+}, which is oxidized to a hypervalent oxoferryl heme a_3 $Fe^{4+}=O^{2-}$. One electron is provided by Cu_B^+, which is oxidized to Cu_B^{2+}, and an electron and proton are believed to be provided by tyrosine 244 (YOH oxidized to $YO^{\bullet}$ radical) [20,21], though another amino acid may be the source of the electron [22]. The 1-electron reduction of P_M generates state F (Fig. 1).

The most detailed studies, with both bovine and bacterial oxidases, have been directed at the F→O transition. The relationship between the electron transfer rate and the rate of voltage generation resulting from the coupled proton movements for the 1-electron reduction of the F state to form the oxidized enzyme (the F→O transition, Fig. 1) has been previously investigated in significant detail with the bacterial [23] and bovine oxidase [24–27], though the absorption and electrometric measurements with bovine oxidase have been made, for the most part, [24,25,28,29] in different laboratories. The electron transfer, monitored by the changes in the heme spectra, occurs in about 1.5 ms, whereas the coupled proton transfer has two phases with τ values of about 1.2 ms and

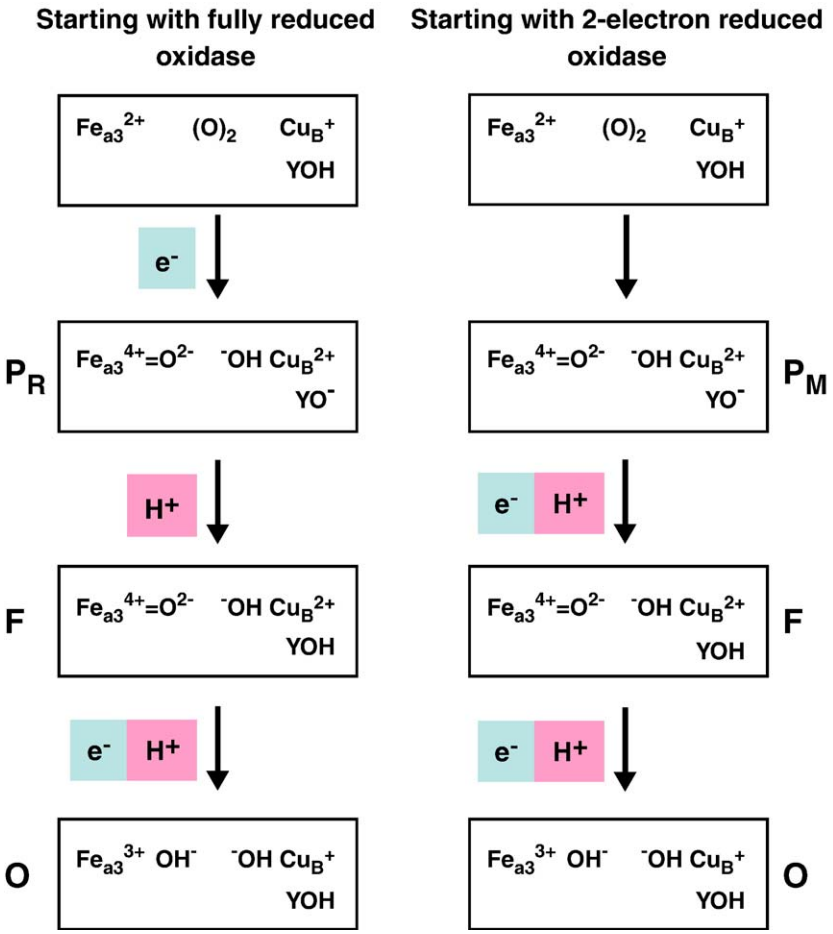

Fig. 1. A schematic showing the postulated states of the heme/copper active site of cytochrome *c* oxidase as the fully reduced (4-electron reduced) enzyme (left side) or the mixed valence (2-electron reduced) enzyme (right side) reacts with O_2. The redox status of the heme a_3 Fe and of Cu_B are shown, along with the redox and protonation state of the active site tyrosine (Tyr244 in the bovine enzyme). In the reaction with the fully reduced enzyme, the P_R product is formed with an electron transfer from heme a, whereas in the reaction with the 2-electron reduced enzyme, an electron is not available from heme a, and an amino acid (presumed here to be Tyr244) is oxidized to form a radical. The conversion to the F state from P_R requires only a proton transfer (presumably from Glu242) but P_M requires both an electron and proton to reach the F state. The proton could be associated with the tyrosine, as pictured here, or could be used to convert the hydroxyl associated with Cu_B to a water.

4.5 ms and relative apparent amplitudes of 1:3. Hence, a portion of the voltage generation is coincident with electron transfer, but the bulk of the charge transfer across the membrane occurs after the electron transfer has been completed [30].

The $P_M \rightarrow F$ transition has been much less investigated than the $F \rightarrow O$ step. Nilsson [31] was the first to study the time-resolved absorption changes of hemes a and a_3 at 445 nm during the single-electron reduction of the P_M state of the bovine oxidase by RuBpy. He reported biphasic oxidation of the photoreduced heme with τ values of 0.27 ms and 4.3 ms and contributions of 40 and 60%. Later, time-resolved studies of membrane potential generation coupled to the P_M–F transition in liposome-reconstituted bovine oxidase were described by Siletsky et al. [24]. The reaction was shown to generate a voltage across the membrane in several kinetic phases. Following the 45 μs electrogenic electron transfer from Cu_A to heme a, the bulk of the voltage is generated by proton movements coupled to cyanide-sensitive electron transfer to the oxygen-reducing site. The time-resolved voltage generation revealed three protonic phases with time-constants of approximately 0.3, 1.3 and 7 ms, which is in reasonable agreement with the absorption measurements of Nilsson [31]. However, no optical controls for electron transfer reactions were made in this work and the P_M states in the two studies were obtained by different methods.

The main purpose of this work is to determine the relationships of the electrogenic proton movements in the $P_M \rightarrow F$ step to the electron transfer from heme a to the heme/Cu active site of the bovine oxidase. The P_M state was prepared by the same method for the two measurements, and the absorption measurements were made at different wavelengths to facilitate the interpretation of the kinetics data.

It is determined in this work that the $P_M \rightarrow F$ transition, measured spectroscopically, occurs about 5-fold more rapidly than the $F \rightarrow O$ transition, 0.3 ms vs. 1.3 ms. Hence, the rapid phase of the voltage generation (0.3 ms) is approximately coincident with the electron transfer, but a significant fraction of the voltage is generated by a slower processes (1.3 ms), similar to the pattern observed with the $F \rightarrow O$ transition [30].

2. Materials and methods

2.1. Materials

Ru_2C [27] is a gift from Russell H. Schmehl (Department of chemistry, Tulane University). 3-CP and aniline are from Sigma. Ru(II)-tris-bipyridyl chloride was purchased from Sigma-Aldrich.

Bovine heart cytochrome *c* oxidase used for the optical experiments was isolated from mitochondria by the modified method of Soulimane and Buse [32] with the introduction of one additional step of gel filtration chromatography. Enzyme concentration was determined from the optical spectra of oxidized enzyme using an extinction coefficient A_{424} of 156 mM^{-1} cm^{-1} [33].

Preparation of bovine cytochrome *c* oxidase for electrometric measurements in Moscow was made as previously described [24], essentially according to [34,35]. The concentration of oxidase used for the electrometric experiments was determined from the absorption difference spectra (dithionite-reduced *minus* ferricyanide-oxidized) using molar extinction value $\Delta\varepsilon_{605-630}$=27 mM^{-1} cm^{-1}.

Cytochrome c oxidase from *R. sphaeroides* modified by a six-histidine affinity tag was purified by chromatography on a Ni-column [36] Purified mitochondrial or bacterial cytochrome *c* oxidase was reconstituted in phospholipid (asolectin) vesicles by a cholate dialysis method [37].

2.2. Time-resolved spectroscopic measurements

In order to obtain the P_M intermediate, oxidized enzyme (~5 μM) in a fluorescence semi-microcuvette was purged with CO under aerobic conditions for about 30 s. Flash-induced absorbance transients at a range of wavelengths from 540 nm to 620 nm with an interval of 3 nm were recorded for 5 ms using 350 μL samples in a 1 cm fluorescence semi-microcuvette. Absorbance changes at 605 nm were recorded for each sample and were used for normalization. Photolysis was carried out with a Phase R model DL 1400 flashlamp-pumped dye laser using LD 490 to produce a 480 nm light flash of 200 ns duration. The total energy per laser flash is approximately 100 mJ. The reaction mixture typically contained 5 μM oxidase, 25–30 μM Ru_2C, 10 mM aniline, 1 mM 3-CP and 0.1% dodecyl maltoside in 5 mM Tris–HCl buffer, pH 8.0. Aniline and 3-CP used as sacrificial electron donors to reduce Ru(III) and prevent electron backflow were quickly added to the cell after complete formation of P_M intermediate and the mixture was flashed. Typically 5 averages were taken for a good absorption transient.

2.3. Time-resolved electrometric measurements

Were made with liposome-reconstituted oxidase from bovine heart or *R. sphaeroides* essentially as described earlier [23,24] with 40 μM RuBpy as the photoactive electron donor for the oxidase and 10 mM aniline as the sacrificial reductant. Liposome-reconstituted cytochrome *c* oxidase attached to one side of a lipid-impregnated collodion film insulating the two compartments of the electrometric cell was converted to the P_M state by gentle bubbling of CO under aerobic conditions as described in the legends to Figs. 2 and 5. Before the treatment with CO, the sample was pre-incubated with ferricyanide and catalase [24]. The difference absorption spectra of liposome-bound oxidase were measured in an SLM-Aminco DW-2000 double beam/dual wavelength spectrophotometer.

2.4. Data analysis

The kinetic traces were resolved into individual exponents using the program "Discrete" [38] and the Microcal Origin 7 software package (Microcal Software, Inc., USA). The relative amplitudes of the individual protonic electrogenic phases were calculated using two different models in which the electrogenic proton transfer processes are assumed to be either independent (parallel model) or sequential (serial model). In the parallel model, the intrinsic amplitudes of the electrogenic steps are simply equal those found by deconvolution of the electrometric curves and have been published earlier [3,23–25,39,40].

The serial model is analogous to the analysis used recently by Medvedev et al. [41], and is based on the sets of Eqs. (4) and (8), derived below by one of us (SAS), for the schemes with two and three consecutive steps, respectively. As the electrogenic phase corresponding to the electron transfer from Cu_A to heme a is very much faster than the subsequent protonic phases, it does not need to be included in the consideration, so the initial state P_0 in Schemes (1) and (5), below, corresponds to the state of the oxidase formed after completion of the electronic phase.

2.4.1. Two-step sequential scheme (Expressions (1)–(4)

We consider a sequence of two irreversible consecutive transitions of the oxidase, $P_0 \rightarrow P_1$ and $P_1 \rightarrow P_2$, that give rise to the fast and slow protonic phases. The two transitions are characterized by intrinsic (genuine) voltage amplitudes V_1 and V_2 and rate constants k_1 and k_2, respectively.

$$P_0 \xrightarrow{k1} P_1 \xrightarrow{k2} P_2 \qquad (1)$$

The time-dependence for the enzyme states P_0, P_1, P_2 (normalized to the total concentration of 1) is:

$$P_0 = e^{-k_1 t};\ P_1 = \frac{k_1}{(k_1 - k_2)}\left(e^{-k_2 t} - e^{-k_1 t}\right);\ P_2 = 1 - P_1 - P_0 \cdot$$

The amplitude of membrane potential, *V*, generated during the reaction sequence (1) can be expressed in terms of enzyme population kinetics (the left part of Eq. (2)). At the same time, the experimentally measured kinetics of the

membrane potential generation is approximated by two exponentials with apparent amplitudes $V_{1,obs}$ and $V_{2,obs}$ (the right part of Eq. (2)), i.e.:

$$V = P_1V_1 + P_2(V_1 + V_2) = V_{1,obs}(1 - e^{-k_1t}) + V_{2,obs}(1 - e^{-k_2t}) \quad (2)$$

After transformations, $V_{1,obs}$ and $V_{2,obs}$ can be expressed as follows:

$$V_{1,obs} = V_1 - V_2\frac{k_2}{(k_1 - k_2)}$$

$$V_{2,obs} = V_2\frac{k_1}{(k_1 - k_2)} \quad (3)$$

Then, the genuine intrinsic voltage amplitudes V_1 and V_2 can be calculated from the experimentally observed amplitudes, V_{obs}, and rate constants, k_1,k_2, from the following set of equations:

$$V_1 = V_{1,obs} + V_{2,obs}\frac{k_2}{k_1}$$
$$V_2 = V_{2,obs}\frac{(k_1 - k_2)}{k_1} \quad (4)$$

2.4.2. Three-step sequentional kinetic scheme (Expressions (5)–(8))

The 3-step sequential model is treated by a procedure fully analogous to that used for the 2-step model above.

$$P_0 \xrightarrow{k1} P_1 \xrightarrow{k2} P_2 \xrightarrow{k3} P_3; \quad (5)$$

where

$$P(0) = e^{-k_1t};$$
$$P_1 = \frac{k_1}{(k_1 - k_2)}\left(e^{-k_2t} - e^{-k_1t}\right);$$
$$P_2 = k_1k_2\left[\frac{e^{-k_1t}}{(k_1 - k_2)(k_1 - k_3)} - \frac{e^{-k_2t}}{(k_1 - k_2)(k_2 - k_3)} + \frac{e^{-k_3t}}{(k_2 - k_3)(k_1 - k_3)}\right];$$
$$P_3 = 1 - P_2 - P_1 - P_0.$$

Then

$$V = P_1V_1 + P_2(V_1 + V_2) + P_3(V_1 + V_2 + V_3)$$
$$= V_{1,obs}(1 - e^{-k_1t}) + V_{2,obs}(1 - e^{-k_2t}) + V_{3,obs}(1 - e^{-k_3t}) \quad (6)$$

and

$$V_{1,obs} = V_1 - V_2\frac{k_2}{(k_1 - k_2)} + V_3\frac{k_2k_3}{(k_1 - k_2)(k_1 - k_3)};$$
$$V_{2,obs} = V_2\frac{k_1}{(k_1 - k_2)} - V_3\frac{k_1k_3}{(k_1 - k_2)(k_2 - k_3)};$$
$$V_{3,obs} = V_3\frac{k_1k_2}{(k_1 - k_3)(k_2 - k_3)}. \quad (7)$$

so that

$$V_1 = V_{1,obs} + V_{2,obs}\frac{k_2}{k_1} + V_{3,obs}\frac{k_3}{k_1};$$
$$V_2 = V_{2,obs}\frac{(k_1 - k_2)}{k_1} + V_{3,obs}\frac{k_3(k_1 - k_3)}{k_2k_1};$$
$$V_3 = V_{3,obs}\frac{(k_1 - k_3)(k_2 - k_3)}{k_1k_2}. \quad (8)$$

In the analysis made by Medvedev et al. [41] an additional parameter β is included, denoting fraction of heme a that is rapidly reduced by Cu_A in accordance with equilibrium distribution of the photoinjected electron between these two redox centers. The remaining fraction of electron, $1-\beta$, remains on Cu_A and is transferred through the heme a into the binuclear centre on a millisecond time scale coupled with proton transfer steps. Accordingly, Medvedev et al. [41] include the voltage formed during this electron transfer into the first protonic component (V_1 in our equations) as a separate additional term, $V_{el}(1-\beta)$, where V_{el} is the "electric" distance between Cu_A and heme a. For most of the cases, the authors assume a value of β=0.5 which corresponds to K_{eq}=1. However, the K_{eq} values measured experimentally by Zaslavsky et al. [27] for the oxidases from *R. sphaeroides* and bovine under conditions very close to those of the current experiments are about 5.4 and 8, respectively (in favor of heme a reduction). This yields β values of 0.84 and 0.89, respectively, i.e. rather close to 1. Accordingly, the $V_{el}(1-\beta)$ term in our results becomes rather small, about 2% and 5% of the overall photoelectric response for the bovine and bacterial oxidases, respectively, and does not significantly affect the calculated intrinsic voltage amplitudes for the protonic phases. Furthermore, the $V_{el}(1-\beta)$ term can actually be distributed among different protonic phases, rather than be simply included in the first protonic phase as assumed in [41]. For these reasons, the $V_{el}(1-\beta)$ term was omitted in the current calculations. If necessary, the intrinsic voltage amplitudes of the protonic phases corresponding to the procedure of Medvedev et al. [41] can be obtained for our data in Tables 1 and 2 by subtracting the above mentioned $V_{el}(1-\beta)$ values from the relative amplitudes of the first protonic phase for the bovine and bacterial enzyme.

3. Results

The P_M state of the bovine oxidase was generated using CO plus O_2 as described in Materials and methods. Curve 1 in Fig. 2 shows the difference spectrum before and after treatment of the oxidized solubilized enzyme with CO in the presence of O_2. The spectrum is typical of the P_M state, and the yield can be estimated to be about 70–75% ($\Delta A_{607-630} \sim 8$ mM^{-1} cm^{-1}) using the $\Delta\varepsilon_{607-630}$=11 mM^{-1} cm^{-1} for the difference spectrum of pure P_M vs. the oxidized state [31]. Similar results have been obtained with liposome-reconstituted oxidase used for electrometric measurements (Fig. 2, curve 2).

Fig. 3 shows the absorption changes monitored at 605 nm and 580 nm over the course of about 5 ms. The 580 nm trace fits to a single exponential with a τ=250 μs. The 605 nm trace is at

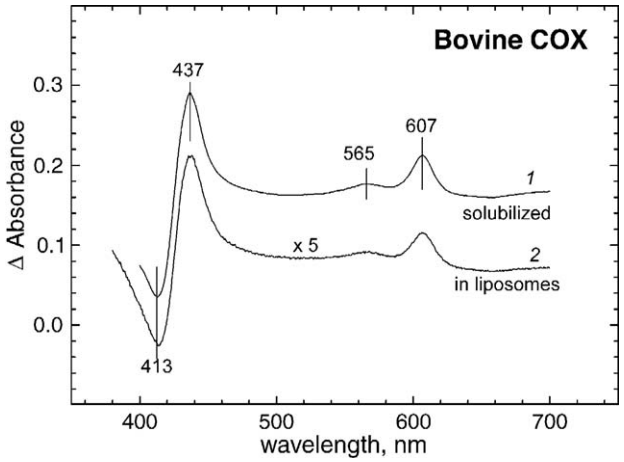

Fig. 2. Difference spectra of the P_M state generated by the CO/O_2 treatment of the solubilized and liposome-bound bovine cytochrome oxidase. For the solubilized oxidase, the solution contained 5–6 μM bovine cytochrome oxidase in 5 mM Tris–HCl, pH 8.0, and 0.1% dodecyl maltoside. For the liposome-reconstituted bovine oxidase, the solution contained 1.2 μM enzyme in 75 mM potassium phosphate buffer, pH 8.0, with 1 mM $MgSO_4$. The sample was pre-incubated aerobically for about 20 min in the presence of 0.1 mM ferricyanide and 10 nM catalase, and the absorption spectrum was taken as an "oxidized" baseline. Subsequently, the sample was gently bubbled with CO for about 60 s, and after several minutes the absorption difference versus the oxidized spectrum was recorded. The difference spectrum has been corrected for the presence of about 5% of the 607 species in the "oxidized" sample, as revealed by electrogenic responses of the "oxidized" sample [24]. The spectrum of the liposome-reconstituted sample has been normalized (5-fold) to match the concentration of the solubilized oxidase in trace 1, for which the absorbance scale applies.

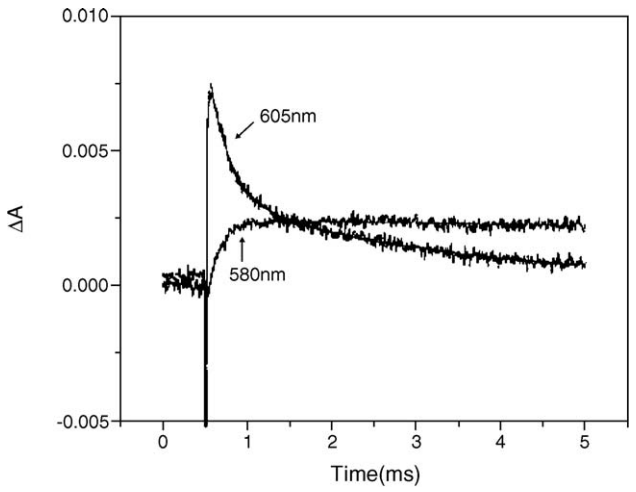

Fig. 3. Kinetics of the absorption changes at 580 nm and 605 nm induced by single electron photoreduction of the P_M state of solubilized bovine oxidase. The sample mixture contained 10 μM bovine oxidase, 30 μM Ru_2C, 10 mM aniline, 1 mM 3-CP in 5 mM Tris–HCl buffer, pH 8.0, with 0.1% dodecyl maltoside. The data show that the rapid phase of absorption decrease at 605 nm matches the formation of the F state (580 nm rise).

least biphasic, with a fast phase (55%) with τ=260 μs and a second, very much slower phase (45%) with τ of about 4.2 ms. These values are in good agreement with the measurements of Nilsson [31], who monitored the spectral changes at 445 nm. Data (not shown) were taken at various wavelengths to determine the spectra associated with these two phases. The difference spectrum of the second phase was consistent with the oxidation of heme a. The significance of this very slow process, also observed by Nilsson [31], is not clear. The 605 nm trace was analyzed taking into account comparable rate constants of heme a reduction by Cu_A (ca. 40 μs) and of its subsequent oxidation (0.2–0.3 ms) by the binuclear site. Using this analysis, it is estimated that the rapid phase of A_{605} decay accounts for 60%–80% of the total, with the remaining 20% to 40% due to the slow (4–6 ms) phase. It is noted, that the absorption decrease at 605 nm due to reoxidation of heme a is overlayed by the decrease in A_{605} associated with the decay of Compound Pm of heme a_3. Due to the overlay of the two processes, the overall trace at 605 nm is expected to go some 30% below zero level (i.e., that observed before the flash), whereas the experimental curve just returns to the zero. The observation is consistent with about 70% of the enzyme undergoing the Pm-to-F transition. As to the slow phase of heme a oxidation, it is not likely to be due to the presence of any contaminating F state being converted to the O state since F is known to be reduced rapidly by CO and is not expected to be present under the conditions used to generate P_M. It is likely that a fraction of the enzyme is in the O state (resting, fully oxidized), however substantial electron transfer from heme a to the binuclear center in the O state is not expected to occur on the <10 ms time scale [24]. Hence, elucidation of the origin of this minor slow phase requires additional experiments. Provisionally, the phase is assigned to some process that is not related to the $P_M \rightarrow F$ transition and the $P_M \rightarrow F$ transition is concluded to be represented in the absorption measurements by a single phase with $\tau \sim 0.3$ ms. However, it cannot be ruled out at this stage that the Pm→F transition does indeed include a minor slow phase, poorly resolved at 580 nm, that may correspond to the minor phase with τ of ca 7 ms resolved in the electric traces [24].

The spectrum derived from the rapid phase is consistent with the enzyme undergoing the $P_M \rightarrow F$ transition in which the 607 nm intermediate of heme a_3 is converted to the 580 nm state concomitantly with partial oxidation of heme a. Conversion of the 607 nm intermediate to the 580 nm state is believed to be associated with the delivery of a proton to the oxygen-reducing site of the enzyme, probably protonating a Cu_B-bound hydroxide to water or perhaps protonating the active-site tyrosinate (Fig. 1). The fact that the rapid phase of heme a oxidation (605 nm trace) is coincident with the monophasic rise of absorption at 580 nm indicates that electron and proton delivery to the active site occur simultaneously. The rate of the optically monitored $P_M \rightarrow F$ transition (about 0.3 ms) is about 5-fold faster than the $F \rightarrow O$ transition measured using the same photoreduction technique (at least 1.5 ms) [27, 31], but it is ca. 3–4-fold slower than the $P_R \rightarrow F$ transition (70–90 μs) measured during the oxidation of the fully-reduced enzyme by oxygen in flow-flash experiments (Fig. 1) (reviewed in [42]).

The rate of formation of the 580 nm intermediate is compared to the time-course of electrogenic proton movements across the membrane in Fig. 4. The rapid phase of vectorial proton transfer (phase 1 in Table 1) is virtually coincident with the optically measured $P_M \rightarrow F$ transition. However, a major portion of the voltage is generated by proton movements that

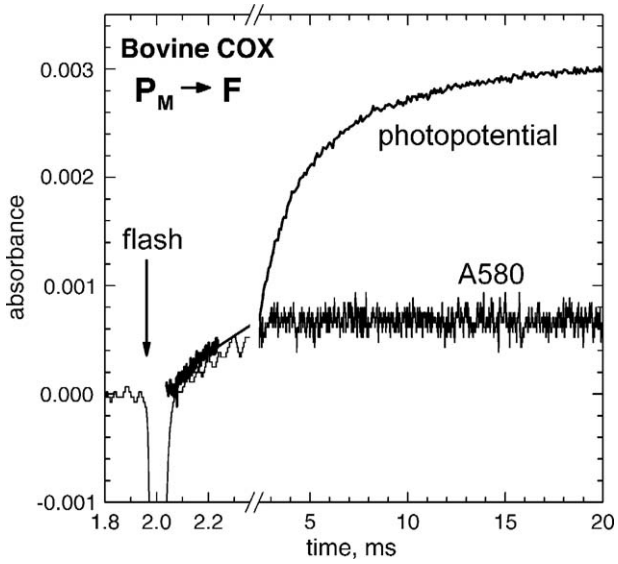

Fig. 4. The kinetics of the $P_M \rightarrow F$ transition, measured by the increase of absorption at 580 nm, compared with the rate of the electrogenic proton transfer that is coupled to the single-electron photoreduction of compound P_M. The rise of absorption at 580 nm and the protonic part of the photoelectric response coupled to the $P_M \rightarrow F$ transition have been normalized by the amplitude of the 0.3 ms phase of the electrogenic proton transfer. The ~15 μs electrogenic phase due to $Cu_A \rightarrow$ heme *a* vectorial electron transfer has been subtracted from the electrometric trace. The electrometric trace has been displaced slightly upwards relative to the absorption trace in order to facilitate comparison of the initial parts of the two curves.

follow the completion of the chemistry at the active site. This is similar to what has been observed for the F→O transition, where a portion of the voltage is generated coincident with electron delivery from heme a to the oxoferryl complex of heme a_3, but a significant part of the photoelectric response takes place after electron transfer [25,27,30].

Characteristics of the electrogenic protonic phases observed in the course of the P_M→F transition are summarized in Table 1 and agree with those published earlier [24]. However, there are important differences as to the interpretation of the observed parameters. As pointed out recently by Medvedev et al. [41], deconvolution of the overall electrogenic responses into individual exponentials gives true time constants of the phases, but the interpretation of the relative amplitudes will depend on the kinetic model employed. If all the electrogenic phases are independent, i.e., start simultaneously at the zero time (parallel model), then the observed amplitudes obtained by deconvolution into exponentials will yield the intrinsic amplitudes of the independent processes. However, if the individual phases are associated with consecutive processes (serial model) then this is not necessarily the case. Incorrect relative amplitudes can result especially when the rates of the processes differ by less than about one order of magnitude [41] (see Materials and methods). For instance, the amplitude of the second (1.3 ms) protonic phase in the P_M→F transition is 2.4-fold larger than that of the fast (0.3 ms) phase when the data are analyzed using the parallel model, but the intrinsic amplitudes of the two phases become rather close to each other in the serial model (Table 1). A similar conclusion was made with respect to the ratio of the two protonic phases observed in the F→O transition of the *R. sphaeroides* oxidase in the analysis by Medvedev et al. [41] of the data in [23]. Therefore, Table 1 gives the amplitudes of the protonic phases and their ratios obtained using both the parallel model and the serial model of the electrogenic processes. It is very likely that the serial model is a more accurate description of the events comprising the proton pump.

The electrogenic response coupled to the P_M→F transition was also measured with the bacterial oxidase from *R. sphaeroides*. Fig. 5 compares the time-course of voltage generation for the P_M→F and the F→O transitions obtained using the same sample of the oxidase-containing proteoliposomes. For the purposes of comparison, the traces have been normalized by the overall amplitude. Characteristics of the electrogenic phases observed in the P_M→F and F→O transitions of the *R. sphaeroides* oxidase are given in Table 2.

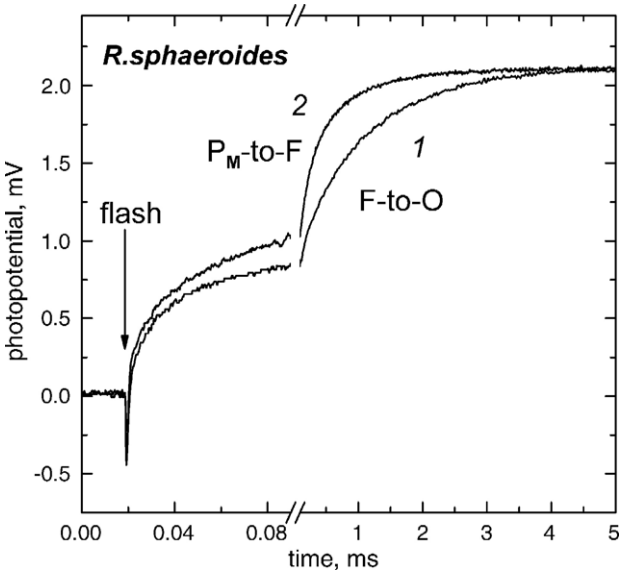

Fig. 5. Comparison of the photoelectric responses of *R. sphaeroides* oxidase associated with the F→O and P_M→F transitions. Liposome-reconstituted wild-type oxidase from *R. sphaeroides* was adhered to the lipid-impregnated collodion film in the electrometric cell. The basic reaction buffer contained 5 mM Tris–acetate, pH 8, with 200 μM ferricyanide to prevent reduction of the oxidase in the dark. 40 μM RuBpy and 10 mM aniline were present to provide for single-electron photoreduction of the oxidase by laser flashes. The sample was treated first with 1 mM H_2O_2 for about 5 min to convert the oxidase to the F state. The laser flash-induced F→O transition was recorded (trace 1) using conditions previously described [23, 39]. After recording trace 1, 10 nM catalase was added to destroy the added H_2O_2 (about 20 min incubation). The sample was then gently bubbled with CO for about 1 min and allowed to stand aerobically for several minutes with stirring to generate the P_M state, using the same procedure employed with the bovine oxidase [24]. Following this, photoelectric trace 2 was recorded. Note that CO efficiently eliminates the residual fraction of the oxidase still remaining in the F state after H_2O_2/catalase treatment. The oxoferryl state undergoes facile 2-electron reduction by CO to the singly-reduced E state [3] which is further oxidized by excess ferricyanide in the mixture to the fully oxidized state of the enzyme, which then reacts with CO and oxygen to generate the P_M state.

Table 1
Electrogenic protonic phases of the P_M→F transition for bovine cytochrome *c* oxidase

Protonic phase	τ, ms	Relative amplitude [a]		
		Parallel model [b]	Serial model [c]	Serial model [d]
1	0.3	1.0 (23%)	1.0 (36%)	1.0 (46%)
2	1.3	2.4 (55%)	1.27 (46%)	1.19 (54%)
3	6.8	1.0 (23%)	0.48 (18%)	0

[a] The amplitude of the rapid protonic phase has been taken as 1. The percent of the overall electrogenic protonic response is given in parentheses.
[b] The relative amplitudes in the parallel model are simply the values resolved by deconvolution of the traces into exponentials.
[c] It is assumed that the 7 ms phase is a third consecutive proton transfer step in the P_M→F transition.
[d] It is assumed that the 7 ms phase is not associated with the P_M→F transition.

The electrogenic pattern of the P_M→F transition in *R. sphaeroides* oxidase is rather similar to that observed for the F→O transition [23, 39]. In addition to the virtually identical microsecond electronic phase with $\tau \sim 13$ μs (not included in the Table 2), two cyanide-sensitive protonic phases are observed with the time constants of 0.18 ms and 0.85 ms. For the bacterial oxidase, the P_M→F transition occurs about twice as fast as the F→O transition, which has τ values of 0.4 ms and 1.54 ms. The faster rate of the P_M→F transition is consistent with the electrogenic pattern of the bovine oxidase. No evidence for a third, slow protonic electrogenic phase analogous to the 7 ms phase in the P_M→F transition the bovine oxidase [24] is observed with the bacterial enzyme.

The ratios of the rapid and slow protonic electrogenic phases are very different for the P_M→F and F→O transitions with the bacterial enzyme. The rapid phase of the P_M→F transition has

Table 2
Photoelectric responses of the $P_M \rightarrow F$ and $F \rightarrow O$ transitions for the oxidase from *R. sphaeroides*

F→O				$P_M \rightarrow F$		
Protonic phase [a]	τ, ms	Relative amplitude [b]		τ, ms	Relative amplitude [b]	
		Parallel model [c]	Serial model		Parallel model [c]	Serial model
1	0.4	1.0 (29%)	1.0 (47%)	0.18	1.0 (61%)	1.0 (70%)
2	1.54	2.5 (71%)	1.12 (53%)	0.85	0.64 (39%)	0.44 (30%)

[a] The protonic phases 1 and 2 in the F→O transition correspond to the so-called *intermediate* and *slow* electrogenic phases as denoted in previous works [3,23,25,39,40].
[b] The amplitude of the rapid protonic phase has been taken as 1. The percent of the overall electrogenic protonic response is given in parentheses.
[c] The relative amplitudes in the parallel model are simply the values resolved by deconvolution of the traces into exponentials.

more than twice the amplitude of the slow phase (Table 2, serial model) whereas, for the F→O transition, the ratio of amplitudes is closer to unity. This differs from bovine oxidase, for which the amplitude ratio of the slow/fast protonic phases is near unity (~1.2) for both the $P_M \rightarrow F$ (Table 1) and F→O steps when the data in [24,25] are re-analyzed according to the serial model.

Finally, it is noted that electrogenic proton transfer coupled to the $P_M \rightarrow F$ transition in the bacterial oxidase is about 2-fold faster than observed for the $P_M \rightarrow F$ transition of the bovine oxidase (Tables 1 and 2). This is similar to the pattern of the electrogenic proton transfers coupled to F→O transition, which is about 3-fold faster in the bacterial oxidases (from either *R. sphaeroides* or *P. denitrificans*) as compared to the bovine oxidase [3,23,39,40].

4. Discussion

4.1. Comparison of the $P_M \rightarrow F$ and F→O transitions

The data presented here show that the rate of electron transfer from heme a to the active site of the bovine oxidase in the P_M state, i.e., the $P_M \rightarrow F$ transition, is 4–5-fold faster than the electron transfer during the F→O step (0.3 ms vs. 1.5 ms). The redox chemistry at the active site is different for these two steps in the reaction cycle, so it is not surprising that they occur at different rates. Most likely, during the $P_M \rightarrow F$ transition, the electron is used to reduce the tyrosine radical to tyrosinate, whereas in the F→O transition, the electron reduces the oxoferryl heme a_3 to the ferric heme ($Fe^{4+}=O^{2-} \rightarrow Fe^{3+}-OH$). In each of these reactions, two protons are thought to be taken up through the D channel from the N-side of the membrane; one proton is delivered to the oxygen-reducing site and one proton is released to the P-side of the membrane. In both the $P_M \rightarrow F$ and F→O transitions, the electron transfer from heme a to the active site occurs approximately simultaneously with a rapid protonic phase of voltage generation, denoted earlier as the *intermediate* electrogenic phase in the F→O studies [25,39], and this is followed by a slower phase of voltage generation.

The relative amplitudes of the two protonic electrogenic phases depend on the model used to interpret the data. As described by Medvedev et al. [41], it is essential to treat the data according to a serial model which proposes that the electrogenic steps are consecutive, rather than simply use the amplitudes as resolved by deconvolution into exponentials, which is correct in general for the parallel model only. Using this analysis, the first two protonic phases with τ values of 0.3 ms and 1.3 ms have amplitudes in a ratio of 1:1.2–1.3 rather than of 1:2.4 as obtained by simple deconvolution (Table 1). The significance and origin of the 7 ms electrogenic phase remains to be established, although it has possible counterparts in the absorption measurements at 445 and 605 nm. Qualitatively, a similar pattern is observed for the F→O transition with the bovine oxidase. Electrogenic proton transfer occurs in two phases with time constants of about 1.2 ms and 4.5 ms, and the first protonic phase (the *intermediate* phase [25,39]) corresponds roughly with the electron transfer to the active site (1.5 ms) (unpublished data of the Moscow group reviewed in [30] and see [25, 27]). The slow proton electrogenic phase is also somewhat larger than the fast protonic phase for the F→O transition. The slow/fast amplitude ratio is about 1.2 when analyzed according to a serial model (Siletsky and Konstantinov, in preparation), which is very close to the value determined in this work for the $P_M \rightarrow F$ transition.

4.2. Assigning the processes resulting in the electrogenic phases

The electron transfer from heme a to the heme a_3/Cu_B active site in the $P_M \rightarrow F$ transition will not directly result in the generation of a transmembrane voltage. The charge movement is parallel to the plane of the membrane. Yet, there is a phase of the voltage generated that is coincident with this electron transfer (0.3 ms). Interpretation of this phase poses an interesting dilemma. On one hand, it is generally assumed that the spectroscopic changes observed in the $P_M \rightarrow F$ transition, i.e. conversion of the 607 nm intermediate to the 580 nm species, is due to protonation of a group at the bimetallic active site [43] and that the proton is transferred from E242 [44]. Electron transfer from heme a does not itself induce the formation of the 580 nm species, as shown by the properties of the P_R state (Fig. 1). It is also likely that proton transfer from E242 will be coupled with very rapid reprotonation of E242 through the D channel [41,45], which is a highly electrogenic process. The slightly electrogenic proton transfer from E242 to the binuclear site, followed by very rapid reprotonation of E242 by D91 through the D channel, could explain the rapid (0.3 ms) protonic electrogenic phase in the $P_M \rightarrow F$ transition. On the other hand, most current models of the proton pump mechanism (but cf. [46]) assume that, at least in the F→O step, electron transfer from heme a to the heme a_3/Cu_B active site is coupled to rapid translocation of a proton from E242 to an acceptor in the exit proton channel (the so-called proton loading site), postulated to be either one of the heme a_3 propionates or a Cu_B-bound histidine [5,7–9,23,47,48]. This step is viewed as "loading" the proton pump, and this proton is then expelled to

the P-phase by coulombic repulsion when the "chemical" proton is delivered to the active site. The postulated proton transfer from E242 to the proton loading site should be electrogenic. Furthermore, this proton transfer would very likely to be followed by immediate electrogenic reprotonation of E242 *via* the D channel [45]. Therefore, this process is also an obvious candidate for the 0.3 ms electrogenic phase. However, it is very unlikely that the 0.3 ms phase of voltage generation in the $P_M \rightarrow F$ step would include both proton transfer from E242 to a proton loading site in the exit channel, as well as the transfer of the chemical proton from E242 to the active site which is responsible for the observed 607 nm → 580 nm conversion. In such a case, the 0.3 ms electrogenic phase would include the transfer of two protons sequentially from E242, with reprotonation in each case through the D channel. This would assign most of the electrogenic proton transfer steps coupled to the $P_M \rightarrow F$ transition to the 0.3 ms phase. Such an interpretation would predict a much larger voltage generation in the 0.3 ms phase and very little voltage generated in the slower 1.3 ms phase, which is not what is observed (Table 1). There are several possible ways to reconcile these considerations.

The first, and probably the simplest, explanation is that the electron transfer (0.3 ms phase) is accompanied only by the transfer of the proton from E242 to the active site (chemical proton) along with the reprotonation of E242, but that the pumped proton is translocated in the slower (1.3 ms) electrogenic step. The second protonic electrogenic phase would then correspond to proton transfer from E242 to either to the proton loading site or to the P-phase, followed by a very rapid second reprotonation of E242 *via* the D channel. The 20%–30% higher amplitude of the 1.3 ms protonic phase relative to the 0.3 ms transient is in good agreement with the transmembrane proton pumping taking place at this step. The assumption that the transfer of the chemical proton precedes that of the pumped proton is consistent with the model of Brzezinski and coworkers [46], but is inconsistent with most prevailing models [5,7,9,23,49] in which it is assumed that the delivery of the chemical proton occurs *after* transfer of the pumped H^+. Furthermore, electrogenic studies of a decoupled N139D mutant of the *R. sphaeroides* oxidase have provided experimental support for the latter proposal [23].

Another way to reconcile the current results with those models [5,7,9,23,49] which assume that the first protonic electrogenic phase includes the transfer of the pumped proton to the proton loading site is to postulate that the formation of the 580 nm state is induced by protonation of the proton loading site, rather than by delivery of the chemical proton to the a_3/Cu_B active from E242. However, recent studies of the reaction of the fully reduced enzyme with O_2 suggest that the proton transfer to the proton loading site can take place prior to and not coincident with the formation of the 580 nm species [8,50].

A third way to reconcile the data is to assume that the proton delivered to the active site does not come from E242 but from a second internal proton donor, and that this proton transfer is not electrogenic. In this way, one can postulate that the 0.3 ms phase of the $P_M \rightarrow F$ transition includes the non-electrogenic proton transfer of this proton to the active site as well as the electrogenic transfer of the pumped proton from E242 to a proton loading site in the exit channel along with reprotonation of E242 *via* the D channel. The putative second internal site would then be reprotonated electrogenically from the N-side of the membrane in the second phase of the reaction (1.3 ms), concurrently with release of the pumped proton from the proton loading site to the P-phase. The problem with this model is that there is no obvious candidate that would serve as a proton donor other than E242.

A fourth way to reconcile the data is to postulate that the immediate reprotonation of E242 is not required (e.g. [46]), despite the theoretical work that indicates this would be energetically impossible [45]. If E242 can remain deprotonated transiently, this would allow one to postulate that E242 is reprotonated only once in the rapid phase and then again in the slow phase. This needs to be explored experimentally.

Finally, it cannot be excluded that the 607 nm → 580 nm optical transition is induced by a rearrangement of the structure/electronic density around the heme a_3/Cu_B site that occurs in response to electron and proton transfers in the 0.3 ms phase and is not due to a specific protonation event.

In summary, there is no unique or obvious assignment of proton transfers to account for the observed amplitudes of the voltage generated in the two phases associated with the $P_M \rightarrow F$ transition. It is quite likely one or more of the assumptions used in building models of the proton pump mechanism is wrong. Indeed, in the discussion above, only those models that include the critical role of the D channel have been considered. Alternative models that emphasize an important role of heme a and/or an alternative proton-conductive H channel in the bovine oxidase, have also been described [49,51–53]. However, the exit part of the H-channel is not conserved in the bacterial oxidases [54,55]. Additional experiments will certainly be needed to sort this out.

4.3. Comparison of the $P_M \rightarrow F$ and the $P_R \rightarrow F$ transitions

The results presented in this work can be compared to the data obtained by studies of the reaction of the fully reduced oxidase with O_2 in the "flow-flash" reaction (see Fig. 1). In the fully reduced enzyme, heme a is reduced at the time when O_2 reacts at the heme a_3/Cu_B active site, and the "fourth" electron required to break the O − O bond is provided by electron transfer from heme a and not by the tyrosine at the active site. It is possible that the P_M state forms as an initial product but, if so, the tyrosine radical must be rapidly reduced by electron transfer from heme a. The reaction product is called the P_R state. The UV-vis absorption spectrum of this state is similar to but not identical with that of P_M [56]. According to the studies of Einarsdóttir and coworkers [57] the operationally defined P_R state may actually be a mixture of 607 nm and 580 nm intermediates with some additional spectroscopic contribution of Compound A (reviewed in [58]). The formation of P_R is followed by the $P_R \rightarrow F$ transition, which is coincident with proton transfer from E242 to the active site [59]. The $P_R \rightarrow F$ step is characterized by τ of 100–140 μs in bacterial oxidase [60,61] and about 80 μs in bovine

oxidase [42,61-63]. The final F state product is identical to the product formed in the $P_M \rightarrow F$ transition, which involves transfer of both an electron and a proton to the heme a_3/Cu_B active site (see Fig. 1). This comparison makes it very likely that the spectroscopic changes which distinguish the F state from the P_M or P_R states are due to protonation of some group at the active site, possibly the protonation of a hydroxide to a water at Cu_B or, as depicted in Fig. 1, protonation of Tyr242 (bovine designation).

The 80 μs time constant of the $P_R \rightarrow F$ step in the bovine oxidase, as measured optically [58], agrees with the monophasic 80 μs electrogenic transient assigned to proton pumping coupled to formation of the F state in bovine enzyme by Helsinki group [64]. It is, therefore, noteworthy that in the single-electron reduction of P_M to F as measured in the current work, there is no evidence for an 80 μs transient observed in either the optical or electric measurements. The fastest phase of the $P_M \rightarrow F$ transition is about 0.3 ms. Furthermore, the $P_M \rightarrow F$ transition includes two, or possibly three, electrogenic protonic phases, in contrast to the single 80 μs protonic electrogenic phase reported for the $P_R \rightarrow F$ step [64]. Obviously, the $P_R \rightarrow F$ transition observed during the oxidation of the fully-reduced bovine oxidase differs significantly from the $P_M \rightarrow F$ step induced by single-electron photoreduction of the P_M state.

It has recently been shown that in the oxidase from *Paracoccus denitrificans*, the formation of the P_R state is accompanied by generation of a transmembrane voltage at the same rate as the electron transfer to the active site and with an amplitude corresponding to charge translocation across only part of the membrane [8,50]. Clearly, this is not due to delivery of a proton from E242 to the oxygen-reducing site, since this would result in the spectroscopic signature of the F state, which is not observed. The electrogenic phase, however, could be due to transfer of the pumped proton from the E242 homologue in *P. denitrificans* to the proton loading site in the exit channel. This suggests that there are two electrogenic steps that occur with the formation of state F in the reaction of the fully reduced enzyme. These correspond to the first two steps shown on the left side of Fig. 1. The second step is the 80 μs phase associated with the $P_R \rightarrow F$ transition [64] . The sum of these two steps can be considered as being equivalent to the two protonic phases of the $P_M \rightarrow F$ transition, described in the current work, and to be the counterparts of the intermediate and slow electrometric phases observed for the photoreduction-induced $F \rightarrow O$ transition [39,40]. If this is correct, then the electrogenic phase coupled to compound F formation in the flow-flash studies [64,65] would follow the same pattern as resolved originally for the $F \rightarrow O$ transition in the photoreduction experiments [25] and observed here for the $P_M \rightarrow F$ step.

5. Conclusions

(1) The electron transfer from heme a to the heme a_3/Cu_B active site in the $P_M \rightarrow F$ transition in bovine oxidase occurs with a time constant of about 0.3 ms.
(2) There is a rapid phase of transmembrane voltage generation ($\tau = 0.3$ ms) that is coincident with the electron delivery to the heme a_3/Cu_B active site of the bovine oxidase. However, at least half of the protonic voltage generation occurs after completion of redox chemistry. This is qualitatively the same sequence of events recorded earlier for the $F \rightarrow O$ transition.
(3) The $P_M \rightarrow F$ transition of the bovine oxidase is about 5-fold more rapid than the $F \rightarrow O$ transition (0.3 ms vs. 1.5 ms) measured using 1-electron photochemical reduction, but 3–4-fold slower than the $P_R \rightarrow F$ step observed in the course of the reaction of O_2 with the fully reduced enzyme (flow-flash reaction).
(4) The $P_M \rightarrow F$ step in the *R. sphaeroides* oxidase is about 2-fold faster than in bovine oxidase, whereas in the reaction of O_2 with the fully reduced oxidase, the rate of the $P_R \rightarrow F$ transition is slower with the *R. sphaeroides* oxidase than with the bovine enzyme.

Acknowledgements

This research was supported by NIH Grants HL16011 (RBG), GM 55807 (MF), GM 20488 (FM and BD) and RR 15569 (FM); Howard Hughes Medical Institute International Scholar Awards 55000320 and 55005615 (AAK), Russian Fund for Basic Research Grant 06-04-48608 (SAS).

References

[1] P. Mitchell, Possible proton motive osmochemistry in cytochrome oxidase, Ann. N. Y. Acad. Sci. 550 (1988) 185–198.
[2] V.Y. Artzatbanov, A.A. Konstantinov, V.P. Skulachev, Involvement of intramitochondrial protons in redox reactions of cytochrome a, FEBS Lett. 87 (1978) 180–185.
[3] M. Ruitenberg, A. Kannt, E. Bamberg, K. Fendler, H. Michel, Reduction of cytochrome *c* oxidase by a second electron leads to proton translocation, Nature 417 (2002) 99–102.
[4] M.I. Verkhovsky, A. Tuukkanen, C. Backgren, A. Puustinen, M. Wikström, Charge translocation coupled to electron injection into oxidized cytochrome *c* oxidase from *Paracoccus denitrificans*, Biochemistry 40 (2001) 7077–7083.
[5] D. Bloch, I. Belevich, A. Jasaitis, C. Ribacka, A. Puustinen, M.I. Verkhovsky, M. Wikström, The catalytic cycle of cytochrome *c* oxidase is not the sum of its two halves, Proc. Natl. Acad. Sci. 101 (2004) 529–533.
[6] M. Wikström, Cytochrome c oxidase: 25 years of the elusive proton pump, Biochim. Biophys. Acta 1655 (2004) 241–247.
[7] M. Wikström, M.I. Verkhovsky, Towards the mechanism of proton pumping by the haem-copper oxidases, Biochim Biophys Acta (2006) in press.
[8] I. Belevich, M.I. Verkhovsky, M. Wikström, Proton-coupled electron transfer drives the proton pump of cytochrome *c* oxidase, Nature 440 (2006) 829–832.
[9] D.M. Popovic, A.A. Stuchebrukhov, Proton pumping mechanism and catalytic cycle of cytochrome *c* oxidase: coulomb pump model with kinetic gating, FEBS Letters 566 (2004) 126–130.
[10] H. Michel, The mechanism of proton pumping by cytochrome *c* oxidase, Proc. Natl. Acad. Sci. U. S. A. 95 (1998) 12819–12824.
[11] P. Mitchell, Chemiosmotic coupling and energy transduction, Glynn Research Ltd, Bodmin, 1968.
[12] S. Ferguson-Miller, G.T. Babcock, Heme/copper terminal oxidases, Chem. Rev. 7 (1996) 2889–2907.
[13] D.L. Rousseau, S. Han, Time-resolved resonance Raman spectroscopy of intermediates in cytochrome oxidase, Methods Enzymol. 354 (2002) 351–368.

[14] S. Han, S. Takahashi, D.L. Rousseau, Time dependence of the catalytic intermediates in cytochrome *c* oxidase, J. Biol. Chem. 275 (2000) 1910–1919.
[15] S. Yoshikawa, K. Shinzawa-Itoh, T. Tsukihara, Crystal structure of bovine heart cytochrome *c* oxidase at 2.8 å resolution, J. Bioenerg. Biomemb. 30 (1998) 7–14.
[16] C. Ostermeier, A. Harrenga, U. Ermler, H. Michel, Structure at 2.7 å resolution of the *Paracoccus denitrificans* two-subunit cytochrome *c* oxidase complexed with an antibody fv fragment, Proc. Natl. Acad. Sci. U. S. A. 94 (1997) 10547–10553.
[17] M. Svensson-Ek, J. Abramson, G. Larsson, S. Tornroth, P. Brzezinski, S. Iwata, The X-ray crystal structures of wild-type and eq(i-286) mutant cytochrome *c* oxidases from *Rhodobacter sphaeroides*, J. Mol. Biol. 321 (2002) 329–339.
[18] T. Soulimane, G. Buse, G.P. Bourenkov, H.D. Bartunik, R. Huber, M.E. Than, Structure and mechanism of the aberrant ba3-cytochrome *c* oxidase from *Thermus thermophilus*, EMBO J. 19 (2000) 1766–1776.
[19] D.A. Proshlyakov, M.A. Pressler, G.T. Babcock, Dioxygen activation and bond cleavage by mixed-valence cytochrome *c* oxidase, Proc. Natl. Acad. Sci. U. S. A. 95 (1998) 8020–8025.
[20] G.T. Babcock, How oxygen is activated and reduced in respiration, Proc. Natl. Acad. Sci. U. S. A. 96 (1999) 12971–12973.
[21] R.B. Gennis, Multiple proton-conducting pathways in cytochrome oxidase and a proposed role for the active-site tyrosine, Biochim. Biophys. Acta 1365 (1998) 241–248.
[22] F.G.M. Wiertz, O.-M.H. Richter, A.V. Cherepanov, F. MacMillan, B. Ludwig, S. de Vries, An oxo-ferryl tryptophan radical catalytic intermediate in cytochrome *c* and quinol oxidases trapped by microsecond freeze-hyperquenching (mhq), FEBS Lett. 575 (2004) 127–130.
[23] S.A. Siletsky, A.S. Pawate, K. Weiss, R.B. Gennis, A.A. Konstantinov, Transmembrane charge separation during the ferryl-oxo → oxidized transition in a nonpumping mutant of cytochrome *c* oxidase, J. Biol. Chem. 279 (2004) 52558–52565.
[24] S. Siletsky, A.D. Kaulen, A.A. Konstantinov, Resolution of electrogenic steps coupled to conversion of cytochrome *c* oxidase from the peroxy to the ferryl-oxo state, Biochemistry 38 (1999) 4853–4861.
[25] D. Zaslavsky, A. Kaulen, I.A. Smirnova, T.V. Vygodina, A.A. Konstantinov, Flash-induced membrane potential generation by cytochrome *c* oxidase, FEBS Lett. 336 (1993) 389–393.
[26] D.L. Zaslavsky, I.A. Smirnova, S.A. Siletsky, A.D. Kaulen, F. Millett, A.A. Konstantinov, Rapid kinetics of membrane potential generation by cytochrome *c* oxidase with the photoactive Ru(ii)-tris-bipyridyl derivative of cytochrome *c* as electron donor, FEBS Lett. 359 (1995) 27–30.
[27] D. Zaslavsky, R.C. Sadoski, K. Wang, B. Durham, R.B. Gennis, F. Millett, Single electron reduction of cytochrome *c* oxidase compund F: resolution of partial steps by transient spectroscopy, Biochemistry 37 (1998) 14910–14916.
[28] R.C. Sadoski, D. Zaslavsky, R.B. Gennis, B. Durham, F. Millett, Exposure of bovine cytochrome *c* oxidase to high triton x-100 or to alkaline conditions causes a dramatic change in the rate of reduction of compound F, J. Biol. Chem. 276 (2001) 33616–33620.
[29] R.C. Sadoski, G. Engstrom, H. Tian, L. Zhang, C.-A. Yu, L. Yu, B. Durham, F. Millett, Use of a photoactivated ruthenium dimer complex to measure electron transfer between the Rieske iron–sulfur protein and cytochrome *c*1 in the cytochrome bc1 complex, Biochemistry 39 (2000) 4231–4236.
[30] A.A. Konstantinov, Cytochrome c oxidase as a proton-pumping peroxidase: reaction cycle and electrogenic mechanism, J. Bioenerg. Biomembranes 30 (1998) 121–130.
[31] T. Nilsson, Photoinduced electron transfer from tris(2,2′-bipyridyl) ruthenium to cytochrome *c* oxidase, Proc. Natl. Acad. Sci. U. S. A. 89 (1992) 6497–6501.
[32] T. Soulimane, G. Buse, Integral cytochrome-c oxidase. Preparation and progress towards a three-dimensional crystallization, Eur. J. Biochem. 227 (1995) 588–595.
[33] G.L. Liao, G. Palmer, The reduced minus oxidized difference spectra of cytochromes a and a3, Biochim. Biophys. Acta 1274 (1996) 109–111.
[34] D.H. Maclennan, A. Tzagoloff, The isolation of a copper protein from cytochrome oxidase, Biochim. Biophys. Acta 96 (1965) 166–168.
[35] L.R. Fowler, S.H. Richardson, Y. Hatefi, A rapid method for the preparation of highly purified cytochrome oxidase, Biochim. Biophys. Acta 64 (1962) 170–173.
[36] D.M. Mitchell, R.B. Gennis, Rapid purification of wildtype and mutant cytochrome *c* oxidase from *Rhodobacter sphaeroides* by Ni^{2+}-NTA affinity chromatography, FEBS Lett. 368 (1995) 148–150.
[37] P.C. Hinkle, Proton translocation by cytochrome c oxidase incorporated into phospholipid vesicles, Methods Enzymol. 55 (1979) 751–776.
[38] S.W. Provencher, A Fourier method for the analysis of exponential decay curves, Biophys. J. 16 (1976) 27–50.
[39] A.A. Konstantinov, S. Siletsky, D. Mitchell, A. Kaulen, R.B. Gennis, The roles of the two proton input channels in cytochrome *c* oxidase from *Rhodobacter sphaeroides* probed by the effects of site-directed mutations on time-resolved electrogenic intraprotein proton transfer, Proc. Natl. Acad. Sci. U. S. A. 94 (1997) 9085–9090.
[40] M. Ruitenberg, A. Kannt, E. Bamberg, B. Ludwig, H. Michel, K. Fendler, Single-electron reduction of the oxidized state is coupled to proton uptake via the K pathway in *Paracoccus denitrificans* cytochrome *c* oxidase, Proc. Natl. Acad. Sci. 97 (2000) 4632–4636.
[41] D.M. Medvedev, E.S. Medvedev, A.I. Kotelnikov, A.A. Stuchebrukhov, Analysis of the kinetics of the membrane potential generated by cytochrome *c* oxidase upon single electron injection, Biochim. Biophys. Acta 1710 (2005) 47–56.
[42] I. Szundi, J.A. Cappuccio, Ó. Einarsdóttir, Amplitude analysis of single-wavelength time-dependent absorption data does not support the conventional sequential mechanism for the reduction of dioxygen to water catalyzed by bovine heart cytochrome *c* oxidase, Biochemistry 43 (2004) 15746–15758.
[43] M. Fabian, G. Palmer, Proton involvement in the transition from the "peroxy" to the ferryl intermediate of cytochrome *c* oxidase, Biochemistry 40 (2001) 1867–1874.
[44] P. Ädelroth, M. Karpefors, G. Gilderson, F.L. Tomson, R.B. Gennis, P. Brzezinski, Proton transfer from glutamate 286 determines the transition rates between oxygen intermediates in cytochrome *c* oxidase, Biochim. Biophys. Acta 1459 (2000) 533–539.
[45] M.H.M. Olsson, P.K. Sharma, A. Warshel, Simulating redox coupled proton transfer in cytochrome *c* oxidase: looking for the proton bottleneck, FEBS Lett. 579 (2005) 2026–2034.
[46] G. Brändén, A.S. Pawate, R.B. Gennis, P. Brzezinski, Controlled uncoupling and recoupling of proton pumping in cytochrome *c* oxidase, Proc. Natl. Acad. Sci. U. S. A. 103 (2006) 317–322.
[47] D.M. Popovic, A.A. Stuchebrukhov, Electrostatic study of the proton pumping mechanism in bovine heart cytochrome *c* oxidase, JACS 126 (2003) 1858–1871.
[48] M. Wikström, M.I. Verkhovsky, G. Hummer, Water-gated mechanism of proton translocation by cytochrome *c* oxidase, Biochim. Biophys. Acta 1604 (2003) 61–65.
[49] S. Papa, N. Capitanio, G. Capitanio, A cooperative model for proton pumping in cytochrome *c* oxidase, Biochim. Biophys. Acta 1655 (2004) 353–364.
[50] C. Ribacka, M.I. Verkhovsky, I. Belevich, D.A. Bloch, A. Puustinen, M. Wikstrom, An elementary reaction step of the proton pump is revealed by mutation of tryptophan-164 to phenylalanine in cytochrome *c* oxidase from *Paracoccus denitrificans*, Biochemistry 44 (2005) 16502–16512.
[51] S. Papa, Role of cooperative H+/e− linkage (redox bohr effect) at heme a/cua and heme a3/CuB in the proton pump of cytochrome *c* oxidase, Biochemistry (Moscow) 70 (2005) 220–230.
[52] S. Yoshikawa, Reaction mechanism, phospholipid structures of bovine heart cytochrome *c* oxidase, Biochem. Soc. Trans. 33 (2005) 934–937.
[53] S. Yoshikawa, A cytochrome *c* oxidase proton pumping mechanism that excludes the O2 reduction site, FEBS Lett. 555 (2003) 8–12.
[54] J. Salje, B. Ludwig, O.M. Richter, Is a third proton-conducting pathway operative in bacterial cytochrome *c* oxidase? Biochem. Soc. Trans. 33 (2005) 829–831.
[55] T.K. H.-M. Lee, D.L. Das, D.A. Rousseau, S. Mills, R.B. Ferguson-Miller, Mutations in the putative H-channel in the cytochrome *c* oxidase from *Rhodobacter sphaeroides* show that this channel is not important for proton conduction but reveal modulation of the properties of heme a, Biochemistry 39 (2000) 2989–2996.

[56] O. Einarsdottir, I. Szundi, N. Van Eps, A. Sucheta, P(m) and P(r) forms of cytochrome *c* oxidase have different spectral properties, J. Inorg. Biochem. 91 (2002) 87–93.
[57] N. Van Eps, I. Szundi, O. Einarsdottir, Ph dependence of the reduction of dioxygen to water by cytochrome *c* oxidase: I. The P(r) state is a pH-dependent mixture of three intermediates, A, P, and F, Biochemistry 42 (2003) 5065–5073.
[58] O. Einarsdottir, I. Szundi, Time-resolved optical absorption studies of cytochrome oxidase dynamics, Biochim. Biophys. Acta 1655 (2004) 263–273.
[59] P. Ädelroth, M. Svensson-Ek, D.M. Mitchell, R.B. Gennis, P. Brzezinski, Glutamate 286 in cytochrome aa3 from *Rhodobacter sphaeroides* is involved in proton uptake during the reaction of the fully-reduced enzyme with dioxygen, Biochemistry 36 (1997) 13824–13829.
[60] P. Ädelroth, P. Brzezinski, B.G. Malmström, Internal electron transfer in cytochrome *c* oxidase from *Rhodobacter sphaeroides*, Biochemistry 34 (1995) 2844–2849.
[61] P. Ädelroth, M. Ek, P. Brzezinski, Factors determining electron-transfer rates in cytochrome *c* oxidase: investigation of the oxygen reaction in the *R. sphaeroides* enzymes, Biochim. Biophys. Acta 1367 (1998) 107–117.
[62] M. Oliveberg, P. Brzezinski, B.G. Malmström, The effect of pH and temperature on the reaction of fully reduced and mixed-valence cytochrome *c* oxidase with dioxygen, Biochem. Biophys. Acta 977 (1989) 322–328.
[63] M.I. Verkhovsky, J.E. Morgan, M. Wikström, Intramolecular electron transfer in cytochrome *c* oxidase: a cascade of equilibria, Biochemistry 31 (1992) 11860–11863.
[64] A. Jasaitis, M.I. Verkhovsky, J.E. Morgan, M.L. Verkhovskaya, M. Wikström, Assignment and charge translocation stoichiometries of the major electrogenic phases in the reaction of cytochrome *c* oxidase with dioxygen, Biochemistry 38 (1999) 2697–2706.
[65] M.I. Verkhovsky, J.E. Morgan, M.L. Verkhovskaya, M. Wikström, Translocation of electrical charge during a single turnover of cytochrome-c oxidase, Biochim. Biophys. Acta 1318 (1997) 6–10.